The characterization of high quality multicrystalline silicon by the electron beam induced current method

2004 J. Phys.: Condens. Matter 16 S211

(http://iopscience.iop.org/0953-8984/16/2/025)

INSTITUTE OF PHYSICS PUBLISHING JOURNAL OF PHYSICS: CONDENSED MATTER

J. Phys.: Condens. Matter **16** (2004) S211–S216 PII: S0953-8984(04)66983-9

The characterization of high quality multicrystalline silicon by the electron beam induced current method

J Chen[1,3], **T Sekiguchi**[1,4], **S Nara**[2] **and D Yang**[3]

[1] Nanomaterials Laboratory, National Institute for Materials Science, Tsukuba 305-0047, Japan
[2] Technical Research Laboratory, Kawasaki Steel Corporation, Mizushima 712-8511, Japan
[3] State Key Laboratory of Silicon Materials, Zhejiang University, Hangzhou 310027, People's Republic of China

E-mail: SEKIGUCHI.Takashi@nims.go.jp

Received 31 July 2003
Published 22 December 2003
Online at stacks.iop.org/JPhysCM/16/S211 (DOI: 10.1088/0953-8984/16/2/025)

Abstract

Multicrystalline silicon (mc-Si) manufactured by a multi-stage solidification control casting method has been characterized by the electron beam induced current (EBIC) method. The average diffusion length of the ingot was over 250 μm, which was much longer than that of conventional mc-Si. The EBIC study revealed that the electrical activities of grain boundaries (GBs) varied with the ingot position due to the impurity contamination level. The main impurity detected was iron. The concentration of iron in the central position was much lower than that at the bottom and top positions. GBs in the central position showed no significant EBIC contrast at 300 K, suggesting low contamination level. GBs in the top and bottom positions, however, showed strong EBIC contrast at 300 K, suggesting high contamination level. At 100 K, a denuded zone with bright contrast developed around GBs in the top and bottom positions. The existence of the denuded zone suggested that impurities were gettered at the GBs. It was considered that the variation of the diffusion length in the ingot was related to the variation of recombination activities of GBs in the different positions, which mainly depended on the impurity contamination.

1. Introduction

Over the last decade, the production of solar cells has increased steadily by an average of 30% per year. In 2001, the world's photovoltaic production reached 396 MW with a 36% increase over 2000. Although crystalline silicon is not the optimal material from the point of view of solid-state physics, over 90% of the world's photovoltaic production is based on the technology of crystalline silicon and it will continue to dominate in the next decade [1]. Among

---

[4] Author to whom any correspondence should be addressed.

0953-8984/04/020211+06$30.00

silicon-based materials, multicrystalline silicon (mc-Si) has become one of the most promising materials in photovoltaic applications due to its low cost and potential for high efficiency. The recorded highest efficiency of mc-Si solar cells has reached 19.8% for 1 cm^2 solar cells [2]. However, the concentration of impurities and crystal defects in mc-Si is significantly higher than that in monocrystalline silicon and strongly suppresses the improvement of the efficiency of solar cells. Past research revealed that the impurities interacted with crystal defects, such as dislocations and grain boundaries (GBs), would introduce deep levels in the band gap and act as strong recombination centres [3–8].

Due to its high spatial resolution, the electron beam induced current (EBIC) method has become a powerful technique for characterizing the recombination properties of crystal defects such as dislocations [6] and stacking faults [7]. EBIC is also suitable for the study of impurity gettering in individual crystal defects. For example, Shen *et al* [8] have studied the effect of copper contamination on the electrical activity of various defects associated with oxygen precipitates in Czochralski silicon by EBIC. Kittler *et al* [9] have applied EBIC to investigate hydrogen passivation and phosphorous gettering in mc-Si materials.

It is well known that the electrical properties of mc-Si materials and the performance of their solar cells were influenced by the crystal growth processes [10–12]. For example, Ehret [13] has compared the crystalline and electrical properties of mc-Si produced by conventional casting and electromagnetic casting (EMC) processes. Mchugo *et al* [14] studied the distribution of impurities in as-grown EMC mc-Si and showed a direct correlation between impurities and regions of high minority carrier recombination.

Recently Nara *et al* [15] succeeded in growing high quality mc-Si by a casting method with a multi-stage solidification control (MUST) process as well as a purification technique. The efficiency of solar cells produced from MUST mc-Si wafers has reached 18.3% with a cell area of 25 cm^2 [16]. In this study, we have investigated the electrical properties of the MUST mc-Si wafers from different solidified positions by means of surface photovoltage (SPV) and EBIC methods.

2. Experimental procedures

A boron-doped p-type (resistivity ~ 0.5–$1.0\ \Omega$ cm) mc-Si ingot grown by the MUST process was used in the experiment. The ingot was about 440 mm × 440 mm × 170 mm in size and 75 kg in weight. The concentration of oxygen and carbon was about 8×10^{16} and 5×10^{18} cm^{-3}, respectively. The main metallic impurities were iron and aluminium, which were detected by atomic absorption spectrophotometry.

The diffusion length of the wafers along the ingot growth direction, i.e. from the bottom (solidified first) to the top (solidified at last), was analysed by the SPV method (FAaST210-SPV). For comparison, conventional cast mc-Si wafers were also checked.

For EBIC observation, samples were cut from three positions of a MUST mc-Si ingot, namely the bottom (1 cm from the bottom side), the centre and the top (1 cm from the top side). All the samples were mechanically ground with carborundum and chemically polished with CP4. Schottky contacts were prepared by aluminium evaporation with a thickness of about 25 nm. EBIC measurements were done with a scanning electron microscope (TOPCON DS-130) in EBIC mode [17]. All observations were done with an electron beam of 20 kV and 2.0 nA. The contrast of EBIC was defined by

$$C = (I_b - I_g)/I_b, \tag{1}$$

where I_b and I_g are the EBIC current collected at background and at GBs, respectively.

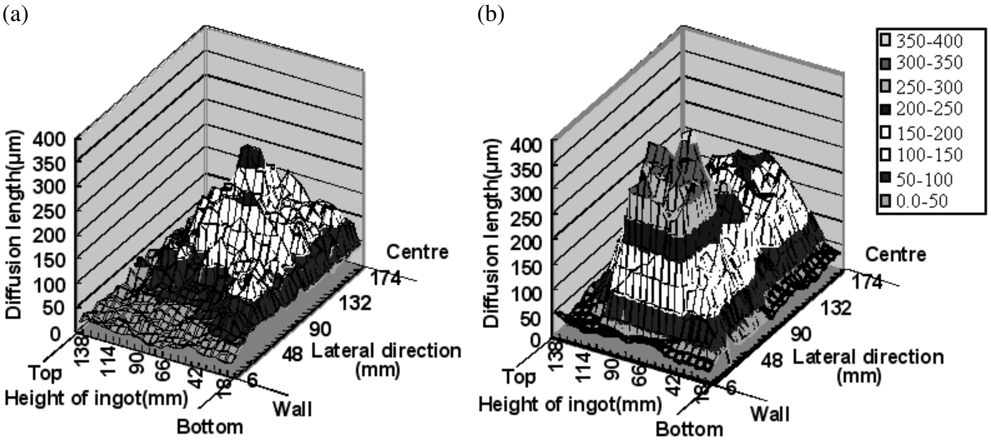

Figure 1. The distribution of the diffusion length of conventionally cast mc-Si ingot (a) and MUST cast mc-Si ingot (b) measured by SPV.

3. Results and discussion

The distribution of the diffusion length along the height and lateral direction of ingot is shown in figure 1. In the central part of the MUST mc-Si ingot, the average diffusion length was about 250 μm and the maximum diffusion length reached 400 μm. It is obvious that the average diffusion length of the MUST mc-Si (figure 1(b)) was much longer than that of the conventional mc-Si (figure 1(a)). Both the MUST and conventional mc-Si ingots show a similar trend in the variation of diffusion length along the height direction, namely the diffusion length in the bottom and the top positions was shorter than that in the central position.

Figure 2 shows the EBIC images of the samples from the bottom, central and top positions of the MUST mc-Si ingot taken at 300 and 100 K. In the central position, no significant EBIC contrast was observed at 300 K, while GBs as well as intragranular defects were visible at 100 K. However, GBs were seen as black lines at both 300 and 100 K in the bottom and top positions. In the images taken at 100 K, a denuded zone, the bright region in the vicinity of GBs, has developed and intragranular defects have become visible. Figure 3 shows the statistics of EBIC contrast at typical GBs marked in figure 2. In the central position, the EBIC contrast of the GB was below the detection limit at 300 K, while it increased up to 25% at 100 K. On the other hand, the EBIC contrast of the GBs in the bottom and top positions did not change so much between 300 and 100 K. From both figures 2 and 3, it is clear that the electrical properties of GBs vary greatly according to the position in the ingot. In addition, there existed two kinds of EBIC contrast distribution at GBs. One was uniform contrast, as seen in the samples from the top and centre positions. The other was dotted contrast, as seen in the bottom position. Such a difference in the EBIC contrast profiles may come from the difference in the GB structures [18].

Since the diffusion length of minority carriers in Si is affected by the recombination centres related to impurities and defects, the variation of the diffusion length and the EBIC contrast along the height direction of the ingot could be explained in terms of the distribution of impurities and defects as well as the interaction between them. The great improvement in the diffusion length in MUST mc-Si compared with that of conventional mc-Si is mainly due to the low concentration of impurities and low density of defects, which was realized by using high purity silicon stock and coating material as well as crucible purification. Most transition

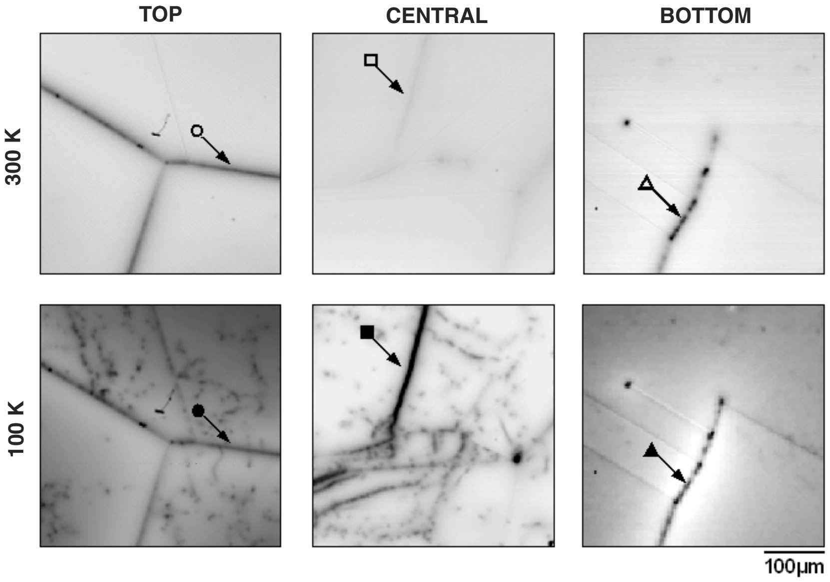

Figure 2. EBIC images of the MUST mc-Si samples from the top, central and bottom positions of an ingot taken at 300 and 100 K.

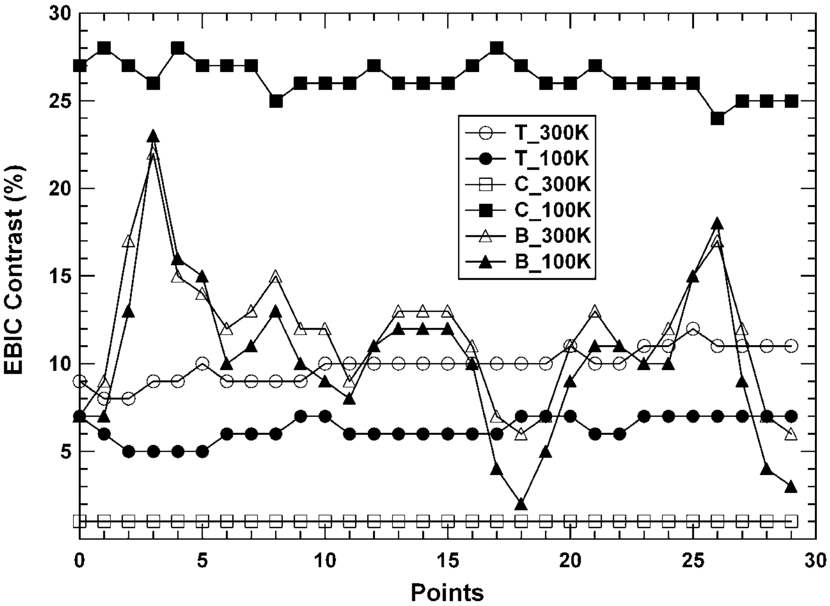

Figure 3. Statistics of the EBIC contrast at GBs in the top, central and bottom positions of the MUST ingot.

metal impurities were below the detection limit except iron. From the atomic absorption spectrophotometry measurement, it was found that the concentration of iron in the central position was below 5×10^{12} cm^{-3}, while that in the top and bottom positions was up to 10^{15}–10^{16} cm^{-3}. The distribution of iron in the ingot was dominated by the diffusion and

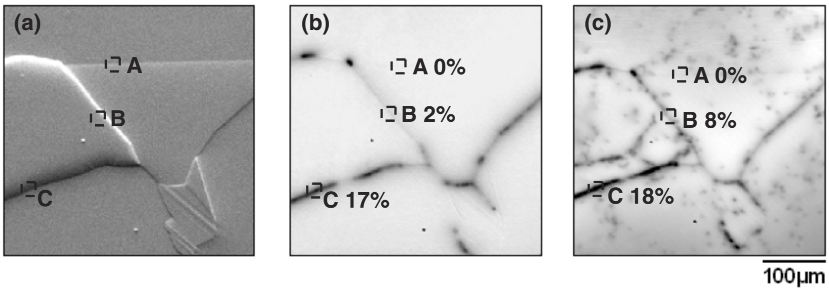

Figure 4. SE and EBIC images of GBs appearing with different EBIC contrasts in the bottom sample. (a) SE (b) EBIC_300 K (c) EBIC_100 K.

segregation of iron atoms. During crystal growth, contamination from the environment, such as the crucible and coating material, as well as the furnace was unavoidable. Impurities, especially iron, would diffuse into the silicon melt and be transferred by convection. During the long time of solidification, the temperature of the ingot was still high enough for iron to diffuse. Since the bottom and side positions of the ingot faced the mould, iron would continue to diffuse into these regions. At the end of crystal growth, the concentration of impurities in the silicon melt increased due to the smaller segregation coefficient. Thus the bottom and top positions had higher concentration of iron than the central, leading to the lower diffusion length in the bottom and top positions (figure 1).

EBIC images (figure 2) of the MUST mc-Si wafers from the top, central and bottom positions were in good accordance with the distribution of the diffusion length (figure 1). The EBIC result reveals that at room temperature contrasts of GBs in the central position were rather weak compared with those in the bottom and top positions. This suggests that GBs in the central position are electrically inactive at room temperature and do not affect the performance of solar cells, while GBs in the bottom and top positions act as recombination centres. The existence of the denuded zone around GBs in the top and bottom positions suggests that impurities were gettered by GBs. Though the diffusion length of those regions near GBs has been improved by the gettering, the average diffusion length in the bottom and top positions was still shorter than that of the central position due to the relatively high concentration of iron atoms. According to the former studies on the electrical property of crystal defects [6, 8, 19] and the Shockley–Read–Hall recombination statistics, it is considered that GBs in the central position are relatively clean and only have shallow levels, while GBs in the top and bottom positions are heavily contaminated and have deep levels.

It should also be noted that in the top and bottom positions, some GBs exhibited weak EBIC contrast, or became almost invisible in the EBIC images, while other GBs exhibited strong EBIC contrast (figure 2). Figure 4 shows the secondary electron (SE) and EBIC images taken at another region in the bottom sample. For a detailed analysis, GBs marked as A, B and C, named as GB_A, GB_B and GB_C, were selected and their EBIC contrasts were compared. GB_A showed no EBIC contrast both at 300 and 100 K. GB_B showed no significant EBIC contrast at 300 K, but it became visible at 100 K with a contrast of about 7%. GB_C showed very high EBIC contrast at around 17–18% at both 300 and 100 K. The variation of EBIC contrast at different GBs in the same position suggests that some GBs appearing with strong EBIC contrast (like GB_C) act as the preferential sites for the gettering of iron, while other GBs with no EBIC contrast (like GB_A) do not act as gettering sites for iron at all. It is considered that the GB structure should play an important role on the gettering of metallic impurities. Further work is needed to study the influence of GB structure on the impurity gettering.

4. Conclusions

High quality MUST mc-Si ingot was studied by means of SPV and the EBIC method. The average diffusion length of the MUST ingot was about 250 μm, which was longer than that of a conventionally grown one. The bottom and the top positions of ingot showed shorter diffusion length than the central position. The EBIC study revealed that the electrical activities of GBs varied according to the position. GBs in the central position were electrically inactive at 300 K while GBs in the top and bottom positions were electrically active. A denuded zone developed around GBs in the top and bottom positions indicating impurities were gettered at GBs. The variation of the diffusion length and the EBIC contrast could be explained in terms of the distribution of impurities and the interaction between impurities and GBs.

References

[1] Goetzbergera A, Heblinga C and Schock H-W 2003 *Mater. Sci. Eng.* R **40** 1
[2] Zhao J H, Wang A H, Green M A and Ferrazza F 1998 *Appl. Phys. Lett.* **73** 1991
[3] Dlamini M D 1996 *Sol. Energy Mater. Sol. Cells* **43** 353
[4] Muller J C and Martinuzzi S 1998 *J Mater. Res.* **13** 2721
[5] Pizzini S 1999 *Phys. Status Solidi* a **171** 123
[6] Kusanagi S, Sekiguchi T, Shen B and Sumino K 1995 *Mater. Sci. Technol.* **11** 685
[7] Sekiguchi T, Shen B, Watanabe T and Sumino K 1996 *Mater. Sci. Eng.* B **42** 235
[8] Shen B, Sekiguchi T, Jablonski J and Sumino K 1994 *J. Appl. Phys.* **76** 4540
[9] Kittler M, Seifert W and Krüger O 2001 *Solid State Phenom.* **78/79** 39
[10] Macdonald D, Cuevas A and Ferrazza F 1999 *Solid-State Electron.* **43** 575
[11] Boudadan J, Monna R, Loghmarti M and Muller J C 2002 *Sol. Energy Mater. Sol. Cells* **72** 381
[12] Sivoththaman S, Laureys W, De Schepper P, Nijs J and Mertens R 1996 *PVSC: The 25th Photovoltaic Specialists Conf.* p 621
[13] Ehret E 1998 *Sol. Energy Mater. Sol. Cells* **53** 313
[14] McHugo S A and Thompson A C 1998 *Appl. Phys. Lett.* **72** 3482
[15] Nara S and Sakaguchi Y 2002 *The 12th Crystalline Silicon Solar Cell Materials and Processes* p 28
[16] Komatsu Y, Takaba Y, Yasukawa S, Okamoto S and Shimizu M 2002 *The 12th Crystalline Silicon Solar Cell Materials and Processes* p 87
[17] Sekiguchi T and Sumino K 1995 *Rev. Sci. Instrum.* **66** 4277
[18] Wang Z J, Tsurekawa S, Ikeda K, Sekiguchi T and Watanabe T 1999 *Interface. Sci.* **7** 197
[19] Radzimski Z J, Zhou T Q, Buczkowski A and Rozgonyi G A 1992 *Appl. Phys. Lett.* **60** 1096